

Citation for published version:

Wansu Lim, Pandelis Kourtessis, Konstantinos Kanonakis, Milos Milosavljevic, Ioannis Tomkos, John M. Senior, 'Dynamic Bandwidth Allocation in Heterogeneous OFDMA-PONs Featuring Intelligent LTE-A Traffic Queuing', *Journal of Lightwave Technology*, Vol. 32 (10): 1877-1885, May 2014.

DOI:

<https://doi.org/10.1109/JLT.2014.2313980>

Document Version:

This is the Accepted Manuscript version.

The version in the University of Hertfordshire Research Archive may differ from the final published version.

Copyright and Reuse:

© 2014 IEEE

Personal use of this material is permitted. Permission from IEEE must be obtained for all other uses, in any current or future media, including reprinting/republishing this material for advertising or promotional purposes, creating new collective works, for resale or redistribution to servers or lists, or reuse of any copyrighted component of this work in other works.

Enquiries

If you believe this document infringes copyright, please contact Research & Scholarly Communications at rsc@herts.ac.uk

Dynamic Bandwidth Allocation in Heterogeneous OFDMA-PONs Featuring Intelligent LTE-A Traffic Queuing

Wansu Lim, Pandelis Kourtessis, Konstantinos Kanonakis, Milos Milosavljevic, Ioannis Tomkos, John M. Senior

Abstract—A heterogeneous, optical/wireless dynamic bandwidth allocation framework is presented, exhibiting intelligent traffic queuing for practically controlling the quality-of-service (QoS) of mobile traffic, backhauled via orthogonal frequency division multiple access-PON (OFDMA-PON) networks. A converged data link layer is presented between long term evolution-advanced (LTE-A) and next-generation passive optical network (NGPON) topologies, extending beyond NGPON2. This is achieved by incorporating in a new protocol design, consistent mapping of LTE-A QCs and OFDMA-PON queues. Novel inter-ONU algorithms have been developed, based on the distribution of weights to allocate subcarriers to both enhanced node B/optical network units (eNB/ONUs) and residential ONUs, sharing the same infrastructure. A weighted, intra-ONU scheduling mechanism is also introduced to control further the QoS across the network load. The inter and intra-ONU algorithms are both dynamic and adaptive, providing customized solutions to bandwidth allocation for different priority queues at different network traffic loads exhibiting practical fairness in bandwidth distribution. Therefore, middle and low priority packets are not unjustifiably deprived in favor of high priority packets at low network traffic loads. Still the protocol adaptability allows the high priority queues to automatically over perform when the traffic load has increased and the available bandwidth needs to be rationally redistributed. Computer simulations have confirmed that following the application of adaptive weights the fairness index of the new scheme (representing the achieved throughput for each queue), has improved across the traffic load to above 0.9. Packet delay reduction of more than 40ms has been recorded as a result for the low priority queues, while high priorities still achieve sufficiently low packet delays in the range of 20 to 30ms.

Index Terms—Passive Optical Network (PON); LTE-A; OFDMA-PON; Wireless backhauling; Quality of Service (QoS); Dynamic Bandwidth Allocation

I. INTRODUCTION

The worldwide explosion of mobile applications and vast

Manuscript received: 17th July, 2013 This work was supported by the ACCORDANCE project, through the 7th ICT Framework Programme.

W. Lim, P. Kourtessis, M. Milosavljevic and J. M. Senior are with Optical Networks Research Group, School of Engineering and Technology, University of Hertfordshire College Lane Campus, Hatfield, AL10 9AB, UK (e-mail: w.lim9@herts.ac.uk).

K. Kanonakis and I. Tomkos are with the High-Speed Networks and Optical Communications Group, Athens Information Technology Center, 19.5km Markopoulou Ave., Peania 19002, Athens, Greece.

adoption of mobile connectivity by end users is fuelling the growth of high-speed global 4G deployments based on long term evolution (LTE) [1-6] standards. Globally, mobile traffic will reach 2,026,121 Terabytes per month in 2017, up from 201,303 Terabytes per month in 2012 [7]. As a result cost-effective optical backhauling links will be eventually required to connect radio cells to a common central office [8-12].

At the same time, orthogonal frequency division multiple access-passive optical networks (OFDMA-PONs) have emerged as a candidate solution for such applications [13-16]. In OFDMA-PONs sub-wavelength resource sharing is performed in the frequency domain using low rate orthogonal subcarriers and not time slots, as it is the case in legacy PONs. Therefore, groups of subcarriers can be dynamically assigned to different optical network units (ONUs) to address their temporal bandwidth requirements in both the upstream and downstream. In the framework of the EU FP7 project ACCORDANCE, several options for back- and front-hauling have been proposed for the convergence of OFDMA-PONs and LTE.

In the front-hauling case, complete layer-2 processing is performed at a central location. On the contrary, the backhauling scenarios of an evolved universal terrestrial radio access network (E-UTRAN) involve evolved node B (eNB) nodes, which are either interconnected or integrated with OFDMA-PON ONUs. Uplink LTE packets received at eNBs are encapsulated within OFDMA-PON packets at the ONUs and then sent via the OFDMA-PON as normal data [17]. The same process takes place in downlink, between the evolved packet core (EPC) and the optical line termination (OLT). The subcarrier assignment is handled by the OLT as for any other OFDMA-PON ONU. Fig. 1 (a) depicts the overall backhauling architecture considered.

With respect to medium access control (MAC) work on converged networks and in particular IP backhauling, existing literature mainly specifies the convergence of Ethernet-PONs (EPONs) with worldwide interoperability for microwave access (WiMAX) [18-20]. Convergences of LTE with next generation PONs (NGPONs) have only been discussed from the architectural point of view, investigating also physical layer impairments at both the optical and wireless domains [21, 22].

In the framework of the ACCORDANCE project, the

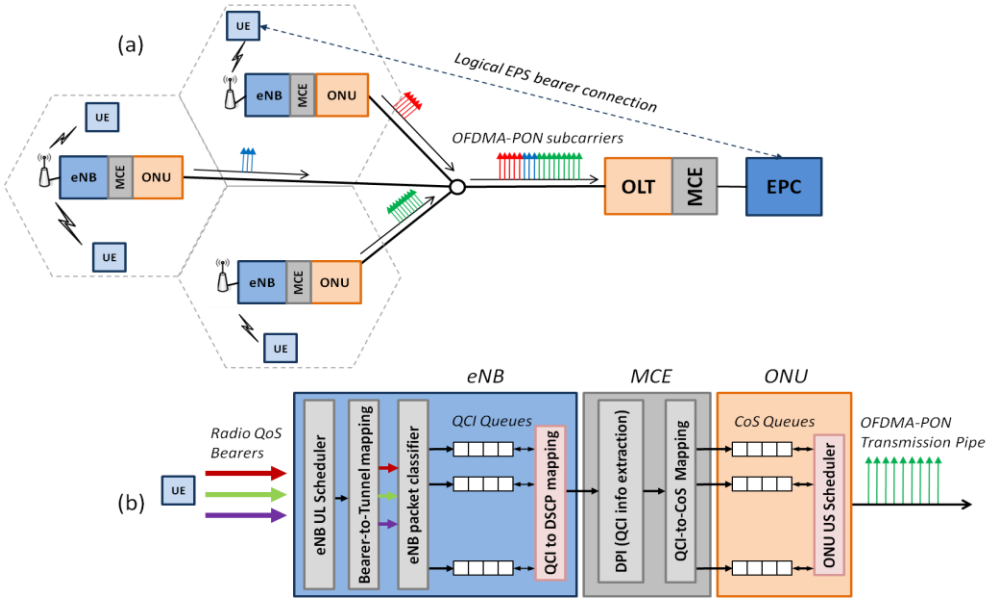


Fig. 1. (a) The considered converged OFDMA-PON and LTE network architecture and (b) the QoS mapping between the eNB and an OFDMA-PON ONU.

mapping of LTE packets to optical queues has been recently presented together with a proposed scheduling scheme [10, 11]. With respect to mapping, the LTE quality of service (QoS) class identifiers (QCIs) were assigned to the OFDMA-PON priorities based on Class of Service (CoS) differentiation. Scheduling involved the allocation of subcarriers to each eNB/ONU ensuring that the bandwidth allocation accounts for the QoS requirements of the respective LTE wireless bearers. This was achieved by allocating subcarriers based on individual queue priorities. Although this scheme provides elevated gain for high priority queues, the performance of the remaining queues is sacrificed due to the limitation of the defined weights to satisfy the whole spectrum of the generated network traffic.

This paper builds on the mapping methodology and algorithms of [10, 11] and extends them to an LTE-A network comprising both wireless user equipment (UEs) and OFDMA-PON residential users. Additionally, a new protocol and inter- and intra-ONU algorithms are proposed in order to optimise the effectiveness of CoS differentiation provided by the bearer mapping. A network topology providing 1Gbps at each eNB/ONU is considered that is also compatible with the foreseen requirements of 5G networks. The new MAC framework proposed combines bandwidth allocation algorithms, performed on the basis of ONU queue priorities, with novel algorithms exploiting weight adaptability, which allow bandwidth allocation to follow closely the actually observed traffic variations.

The details of the heterogeneous protocol are given in section II and III with respect to the mapping strategy, OFDMA-PON control framework and weighted subcarrier allocation concept. The paper progresses by describing in detail the proposed algorithms in section IV, followed by their performance evaluation via elaborate end-to-end converged network simulations in Section V. Finally, conclusions are drawn in Section VI.

II. QoS MAPPING BETWEEN LTE AND OFDMA-PONS

The QoS model of the evolved packet system (EPS) for LTE, which was standardized in 3GPP [23], is based on the logical concept of an EPS bearer [24]. An EPS bearer uniquely identifies packet flows that receive the same packet forwarding treatment between UEs and the EPC [25]. Unlike LTE, standardised PONs (including the OFDMA protocol designs developed in FP7 ACCORDANCE) do not support bearer-based connections. Bandwidth requests are queue-oriented instead. To achieve a truly integrated scheduler, an effective mapping mechanism is therefore required between the OFDMA-PON priority queues and the LTE bearer. In particular, mapping has to identify which LTE bearer should be stored in which OFDMA-PON priority queue for achieving the equivalent QoS. Moreover, in terms of the number of QoS queues, the OFDMA-PON would normally account for a different number of priority queues at each ONU (e.g. three are considered in this work) compared to the eight standardized QCIs of LTE. In this work, we follow a similar mapping approach to the one we proposed in [10]. As shown in Fig. 1 (b), after the received UEs IP packets are mapped to the mobility tunnels based on their bearer ID and classified to appropriate QCIs [25], mapping is conducted by a Mapping Controller Element (MCE) residing either between the eNB and the ONU (in the uplink) or between the EPC and the OLT (in the downlink). The MCE first performs Deep Packet Inspection (DPI) to extract the QCI information from the arriving packets and then consults a predefined mapping table to decide on the CoS for each packet. Depending on the number of queues at each side and the requirements of each individual QCI queue, it is possible to either group multiple QCI queues to a single CoS queue, or even have a 1-1 mapping among them.

III. THE CONSIDERED OFDMA-PON CONTROL FRAMEWORK AND WEIGHTED DYNAMIC SUBCARRIER ASSIGNMENT

As soon as the QCI-CoS mapping has been completed, it must be ensured that the OFDMA-PON MAC bandwidth allocation mechanism is performed in such a way that takes into account the QoS requirements of the respective LTE wireless bearers. Dedicating one or more whole subcarriers to each CoS could lead to inefficient utilization of resources, since the subcarrier capacity is typically in the range of few tens of Mbps. Therefore, packets sent by the ONU (or OLT) scheduler use the single transmission pipe formed by all upstream subcarriers assigned to the ONU.

The MAC control signaling for dynamic bandwidth assignment assumed is similar to what is described in [26]. The OLT sends GATE messages to each ONU once every T_s (scheduling cycle), assigning an upstream subcarrier range (transmission pipe) which can be applied from the next upstream cycle on. In the downstream this is achieved using RX_CONFIG messages. At the end of each cycle, ONUs send an upstream REPORT message with the number of bytes in each of their OFDMA-PON CoS queues.

The Dynamic Subcarrier Assignment (DSA) algorithm [10] operates as follows: Let $B_{i,j}^{k-1}$ denote the number of bytes reported by ONU i for CoS queue j in cycle $k-1$. Then, the number of subcarriers assigned to ONU i in cycle k will be:

$$S_i^k = S_{i,g} + \frac{\sum_j B_{i,j}^{k-1}}{\sum_{i,j} B_{i,j}^{k-1}} \cdot \left(S - \sum_i S_{i,g} \right) \quad (1)$$

S is the total number of upstream subcarriers and $S_{i,g}$ the number of guaranteed upstream subcarriers for ONU i . For the downstream the same equation can be used, where $B_{i,j}^{k-1}$ denotes this time the number of bytes arrived at the downstream queue of the OLT for ONU i for CoS queue j in cycle $k-1$.

However, since the transmission pipes allocated to each ONU/eNB in the upstream/downstream directions are to be shared by all CoS queues, it is crucial to select their size in such a way that fairness across traffic priorities throughout the whole network is ensured. For example, the QoS of high-priority bearers served by an ONU/eNB with a low aggregate traffic volume could be compromised, since such an ONU/eNB may get assigned a lower number of subcarriers.

For this reason, in [10] we also proposed a Weighted Dynamic Subcarrier Assignment (WDSA) scheme. A weight w_j is assigned to each CoS, and then Eq. (1) is used, using modified values as follows: $B_{i,j}^{k-1} = w_j \cdot B_{i,j}^{k-1}$. As a result, the ONUs with the higher representation of high priority traffic are assigned a relatively higher number of subcarriers even if their aggregate traffic is not high. The work in [11] further reported on the performance evaluation of the WDSA algorithm and its comparison to algorithms not benefiting from a weight-specific scheduler.

IV. HYBRID DYNAMIC SUBCARRIER ASSIGNMENT WITH ADAPTABLE WEIGHTS

Although the WDSA scheme described above provides the

tools for handling the QoS differentiation requirements of both residential and mobile traffic, it comes with some drawbacks. First of all, the weight distribution is static while the actual traffic patterns for the different priorities are expected to vary over time, making it difficult to select a single optimal set of weights. Moreover, unfairness may appear if there is significant priority mix discrepancy among different ONUs. For example the performance of CoS1 for an ONU producing only this kind of traffic will be worse than the CoS1 of another ONU which also produces high priority traffic (CoS0) – even if the latter ONU produces the same amount of CoS1 traffic.

For these reasons, this paper introduces a new scheme aiming to increase fairness between the high and low/middle priority queues. First of all, we propose a hybrid way of operation which allows automatically switching between an adaptively weighted DSA (AWDSA) and a non-weighted DSA scheduler (i.e. a scheduler with practically the same weight for each priority queue). The latter is expected to be particularly beneficial to the performance of the middle and lower packet queues.

TABLE I. DBA ALGORITHM PARAMETER NOTATIONS

	Variable	Description
	N	Number of ONUs
	\mathfrak{R}^k	Subcarrier grouping ratio in cycle k
Inter-ONU scheduling specific parameters	$w_{i,j}^k$	Weight for ONU i , for CoS $j=0,1,2$
	S_{DSA}^k	Subcarrier pool for DSA scheme
	S_{AWDSA}^k	Subcarrier pool for AWDSA scheme
	S	Total number of upstream subcarriers
	$S_{i,g}$	Guaranteed subcarriers
	S_i^k	Allocated subcarriers for ONU i
Intra-ONU scheduling specific parameters	M	Number of priority queues
	R_i^k	DSA allocated bandwidth over total allocated bandwidth for ONU i
	$\psi_{i,j}^k$	Weight for ONU i , CoS j
	B_{DSA}^{intra}	Bandwidth allocation using DSA scheme
	B_{AWDSA}^{intra}	Bandwidth allocation using AWDSA scheme
	Q_j	Allocated bandwidth for CoS j
General parameters	G_j^i	Ratio of the requested and allocated bandwidth of ONU i for CoS queue j
	α	Adaptation step of \mathfrak{R}^k and R_i^k
	β	Adaptation step of $\psi_{i,j}^k$ and $w_{i,j}^k$
	$B_{i,j}^k$	Requested bandwidth for ONU i , CoS j
	D_{sc}	Data rate of a single subcarrier in bps
	T_s	Polling cycle time

Under this scheme, the available subcarriers in the network are split into two, dynamically re-organized groups, each controlled by the AWDSA and DSA algorithm respectively. To be able to split the network subcarriers into two groups, a new parameter was introduced in the inter-ONU scheduler in OLT, which we call the subcarrier grouping ratio, \mathfrak{R}^k . For clarity Table I provides all parameters included in equations (1) to (11), describing the new bandwidth allocation methodology and the associated notation. The subcarrier grouping ratio defines the ratio of subcarriers being used by the non-weighted algorithm over the total number of available subcarriers and ranges between 0 and 1 (i.e. a value of 0 denotes that all subcarriers are allocated using AWDSA, while and 1 means that bandwidth allocation is based purely on DSA). Intelligent traffic queuing is implemented in the new scheme by automatically resetting

the subcarrier grouping ratio value depending on the actual traffic trend. This is performed by the OLT at every polling cycle during the exchange of REPORT messages, exploiting the difference in required bandwidth between consecutive cycles for each queue. For example, in case the required bandwidth in cycle k for the highest priority queue is greater than in polling cycle $k-1$, the subcarrier grouping ratio is reduced and therefore the number of subcarriers available for AWDSA is increased ($S_{AWDSA}^k > S_{DSA}^k$). The scheme operates similarly for the middle and low priority queues.

The equation used for the calculation of the subcarrier grouping ratio is given below:

$$\mathfrak{R}^k = \begin{cases} (1 - \alpha) \cdot \mathfrak{R}^{k-1}, & \text{if } (B_{i,j=0}^k > B_{i,j=0}^{k-1}, B_{i,j=1,2}^k < B_{i,j=1,2}^{k-1}) \\ (1 + \alpha) \cdot \mathfrak{R}^{k-1}, & \text{if } (B_{i,j=0}^k < B_{i,j=0}^{k-1}, B_{i,j=1,2}^k > B_{i,j=1,2}^{k-1}) \end{cases} \quad (2)$$

where α represents the adaptation step of the subcarrier grouping ratio.

With the subcarrier grouping ratio calculated, for each polling cycle, the subcarrier pools are formed using the expressions below:

$$S_{DSA}^k = \left[\left(S - \sum_i S_{i,g} \right) \times \mathfrak{R}^k \right] \quad (3)$$

$$S_{AWDSA}^k = S - S_{DSA}^k \quad (4)$$

Intelligent traffic queuing is further enhanced in the proposed algorithm by means of adaptable weights, being able to optimize for each ONU the allocation of subcarriers to each of their queues. The bandwidth calculation takes place by considering consecutive polling cycles and since subcarriers can be assigned only from within those already available in the subcarrier pool, the weight distribution (and therefore the bandwidth allocation) for the next cycle is performed based on queue priority. The following expression (5) describes the weight adjustment process for each ONU and CoS:

$$w_{i,j}^k = \begin{cases} (1 - \beta) \cdot w_{i,j}^{k-1}, & \text{if } (B_{i,j}^k < B_{i,j}^{k-1}) \\ (1 + \beta) \cdot w_{i,j}^{k-1}, & \text{if } (B_{i,j}^k \geq B_{i,j}^{k-1}) \end{cases} \quad (5)$$

where β is the weight adaptation step.

The number of subcarriers assigned to ONU i in cycle k is consequently given by:

$$S_i^k = S_{i,g} + \frac{\sum_j (B_{i,j}^{k-1} \times w_{i,j}^k)}{\sum_{i,j} (B_{i,j}^{k-1} \times w_{i,j}^k)} S_{AWDSA} + \frac{\sum_j B_{i,j}^{k-1}}{\sum_{i,j} B_{i,j}^{k-1}} S_{DSA} \quad (6)$$

In contrast to the use in [10] of strict priority scheduling, with respect to the order of service among the individual CoS queues in each ONU, a different approach is introduced in this paper to avoid starvation of lower priority queues. High priority queues still transmit their data first, to satisfy the requirements for real-time services and intense bandwidth provision, with the distinctive difference that middle and low priority queues are also allocated time intervals to be able to transmit data within the same polling cycle. Intra scheduling is therefore

implemented in two steps. Initially (7) and (8) provide the bandwidth assigned to each ONU queue in bytes for the non-weighted and weighted algorithms respectively. These are distinguished by the newly introduced parameter, R_i^k , as opposed to \mathfrak{R}^k used for inter-ONU scheduling, that is the DSA allocated number of bytes over the total bytes for ONU i .

$$B_{DSA}^{intra} = S_i^k \times D_{sc} \times T_s \times R_i^k / 8 \quad (7)$$

$$B_{AWDSA}^{intra} = S_i^k \times D_{sc} \times T_s \times (1 - R_i^k) / 8 \quad (8)$$

D_{sc} and T_s denote the rate of a single subcarrier in bits per second and the duration of each polling cycle respectively. Subsequently, depending on the bandwidth required by each ONU for each of their queues, the intra-ONU weight distribution per queue, $\psi_{i,j}^k$, is also dynamically adapted by solving (5) with respect to $\psi_{i,j}^k$ rather than $w_{i,j}^k$. Therefore, when an ONU receives a GRANT message, each priority is assigned their own number of bytes, as given by:

$$Q_j = B_{AWDSA}^{intra} \frac{B_{i,j}^k \times \psi_{i,j}^k}{\sum_j (B_{i,j}^k \times \psi_{i,j}^k)} + B_{DSA}^{intra} \frac{B_{i,j}^k}{\sum_j B_{i,j}^k} \quad (9)$$

Q_j defines the maximum transmitting bits assigned to CoS queue j .

It is worth mentioning at this point that fairness has been previously referred to in [27, 28] and a fairness index ($0 < f < 1$) has been measured. The bandwidth granted to each ONU as a whole was used in these measurements though, providing an evaluation of fair distribution of the available bandwidth to network ONUs. In order to evaluate the fairness of bandwidth allocation to individual priority queues and not to ONUs we have adapted the definition of the fairness index f of the proposed heterogeneous scheme as follows:

$$f = \frac{\sum_{i=1}^N \left(\frac{(\sum_{j=1}^M G_j^i)^2}{M \times \sum_{j=1}^M (G_j^i)^2} \right)}{N} \quad (10)$$

where M and N are the number of priority queues and ONUs respectively. G_j^i represents the ratio of the requested and allocated bandwidth of ONU i for CoS queue j , defined by:

$$G_j^i = \frac{Q_j}{B_{i,j}^k} \quad (11)$$

V. PERFORMANCE EVALUATION

The complete network evaluation was performed in OPNET by the integration in a single simulation platform of wireless user equipment, developed in C to demonstrate a practical LTE-A network and a custom made OFDMA-PON incorporating the proposed mapping and scheduling algorithms. A fully functional 3GPP, LTE-A network model was developed, supporting 16 cells with 10 UEs per cell featuring an inter site distance (ISD) of 500m and 50km/h UE mobility. The

simulated backhaul OFDMA-PON network exhibits 1024 subcarriers, 20km reach, 16 eNB/ONUs, 16 residential ONUs and 40Gbps aggregate capacity, while three optical packet priorities (high, middle and low) were specified. The buffer size of each ONU queue is limited to 1Mbyte with the grant processing and propagation delays set to $5\mu\text{s}$ and $5\mu\text{s}/\text{km}$ respectively. Each eNB/ONU is aggregated to 1Gbps, in accordance with LTE-A, corresponding to a total data rate from all eNB/ONUs combined of 16Gbps. This figure represents 40% of the feeder fibre traffic. It should be noted that the aggregate wireless traffic load from an eNB antenna uplink is kept constant in the simulation while the residential traffic load is varied. This is a valid hypothesis since the proposed network is evaluating the effect of residential NGPON users on LTE-A where constant aggregate wireless traffic of 1Gbps represents the worst case scenario (e.g. dense urban environments with high radio cell capacities). It is expected that with lower wireless traffic loads the general performance will be improved and therefore it is not necessary to be further explored in this paper.

Each UE manages five bearers, QCI 5, QCI 1, 2 and QCI 6, 7 grouped to represent the equivalent high, middle and low priority wireless packets respectively. These priorities occupy 20%, 40% and 40% of the total generated packets [10, 11]. Regarding QCI-to-CoS mapping, QCI 5 is mapped to CoS0 (high priority), QCI 1, 2 to CoS1 (middle priority) and QCI 6, 7 to CoS2 (low priority). ON-OFF traffic is generated, with periods exhibiting an exponential distribution with a mean of $500\mu\text{s}$. The packet inter-arrival time within ON periods is implemented by a Pareto distribution to generate bursty traffic. The packet size is uniformly generated between 64-1500Bytes.

As a first step, simulation results are drawn to define the network performance following the application of a hybrid, weighted and non-weighted algorithm with adaptive weights, DSA, as well as a WDSA displaying only fixed weights. In the scenario fixed weights are used, these are implemented by setting the weights of high, middle and low CoS queues to 10, 5 and 2 respectively, being consistent with previously drawn results [10, 11], while maximizing the data transfer flow in favor of the high priority traffic. The same distribution is used by ONUs for intra CoS queue scheduling. The total number of guaranteed subcarriers, $S_{i,g}$ in each scenario is 160, allowing the remaining 864 subcarriers to be dynamically allocated to ONUs.

Fig. 2 draws the fairness index for the hybrid, fixed-weight (WDSA) and DSA scenarios. The offered load axis represents the total amount of traffic generated by each residential ONU. At an offered load of 1.0, each residential ONU generates 1.5Gbps, corresponding to 24Gbps total residential traffic (24Gbps = 16 residential ONUs \times 1.5Gbps). Important to be reminded at this stage is that the traffic generation of each eNB/ONU is aggregated to 1Gbps, corresponding to 16Gbps total wireless traffic, included in the calculation and performance evaluation of the residential users. Therefore at the traffic load of 1.0, the total generated network traffic is aggregated to 40Gbps.

The hybrid algorithm in Fig. 2 displays an increased degree

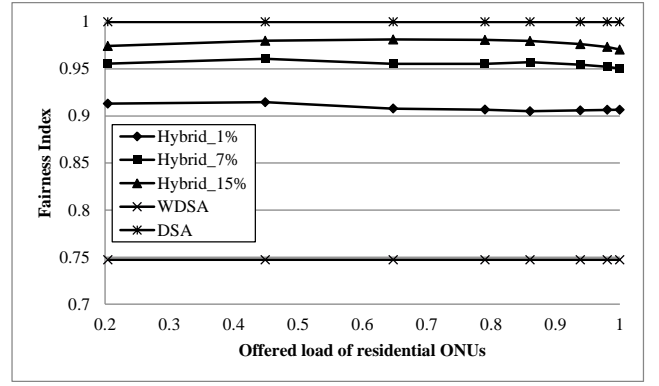


Fig. 2. Fairness index for the hybrid, WDSA and DSA algorithms.

of fairness, justifying the more accurate distribution of bandwidth among priority queues. This can be explained if it is considered that the subcarrier grouping ratio and weights are flexibly responding to the changing traffic conditions. As a result the fairness index of the adaptive algorithm in every case is above 0.9. The percentages in the legend of Fig. 2 represent the adaptation step (by the same amount both up or down) of the subcarrier grouping ratio, α and weights, β , that define the adaptability of the inter- and intra-ONU schedulers. It has been particularly observed that in the case of the hybrid_15% fairness reaches its highest value of almost 1. In this case, 15% describes an extended adaptation step in the allocated bandwidth that has shifted from the high priority queues to middle and low priority queues. As derived from (2) and (5) changing bandwidth requirements will result automatically in subcarrier and weights to increase or decrease between cycles by the same percentage, increasing therefore the overall fairness.

To give an example, \mathfrak{R}^k and R_i^k as well as weights $w_{i,j}^k$ and $\psi_{i,j}^k$ are set to 0.5 and 10:5:2 respectively at the beginning of the simulation. In the case of 7%, both \mathfrak{R}^k and R_i^k continuously increase and decrease by 0.07, depending on the temporal traffic conditions during the simulation. The upper and lower bounds are 1 and 0 respectively. With \mathfrak{R}^k of 0.57 at the moment the pool of the DSA and AWDSA may contain 492 (0.57×864) and 372 subcarriers respectively from (3) and (4). With respect to the changing weights, the initial fixed distribution of 10, 5 and 2 is corresponding to 58.8%, 29.4% and 11.8% bandwidth occupancy and in the case of the 7% adaptation step each weight can be changed positively or negatively using (5). Following this calculation as the adaptation step increases, the adjustable range of the subcarrier grouping ratio and each weight increases.

The performance of the WDSA algorithm is also shown in Fig. 2. The traffic generation pattern, as described earlier in this section, used for each queue priority, corresponds to bandwidth being allocated depending closely on the fixed distribution of weights other than the requested bandwidth [10, 11]. In that case the normalized Q_j^{Nml} , derived from (9), is given by $(TG_j \times w_j) / \sum_j (TG_j \times w_j)$, for each priority and results to 0.416, 0.416 and 0.168 for Q_0^{Nml} , Q_1^{Nml} and Q_2^{Nml} respectively.

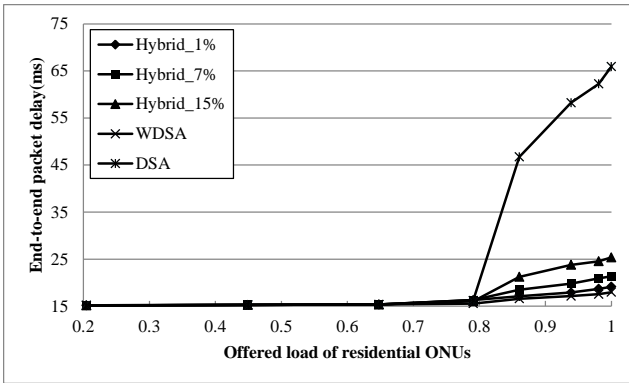


Fig. 3. End-to-end packet delay for CoS0 traffic.

For intra-scheduling, WDSA uses only the first term of (9), implying that the allocated bandwidth of each queue depends on their requested bandwidths as well as weights and therefore the parameter (G_j^i) of the fairness index calculation, given by (11), results to: $G_0^i = 2.08$, $G_1^i = 1.04$, $G_2^i = 0.42$. Therefore, based on analysis the fairness index given by (10) is equal $f=0.748$. This figure is in close agreement with the measured simulation results for WDSA supporting the validity of the model. In addition, the fairness index of DSA algorithm is 1 because the allocated bandwidth to each queue is sufficient to satisfy their individual bandwidth needs. This is demonstrated by (11) where the ratio G_j^i will be always 1 regardless of the queue priority.

Fig. 3 exhibits the end-to-end packet delay of CoS0. Five experimental scenarios have been simulated, as before, to draw the performance trend following the adaptation step of the subcarrier grouping ratio and weights. As shown in Fig. 3, at traffic loads below 80% of the total generated load, the packet delay figures of the hybrid schemes are in agreement, as well as with the WDSA algorithm. This performance can be justified, considering that for the AWDSA the high priority queue is naturally supported all the way across the network load, by means of a greater assigned weight, while in the hybrid algorithms there are still enough subcarriers to be able to fully support the bandwidth request for CoS0. However, for the ever increasing traffic above 80%, adaptive weights start experiencing higher delays. This is because any adaptation step on the subcarrier grouping ratio and weight parameters in the hybrid algorithm perform in favor of the non-weighted scheduler and as a whole, in comparison to WDSA, CoS0 might not have access to the amount of bandwidth being allocated before. This characteristic is not expected to impose a threat in the converged network. The first reason is that it occurs while in parallel there is an improvement, as it is confirmed by Fig. 6 for the low priority packets. Also significantly in the presence of the hybrid protocol the network can be automatically optimized to the adaptation step percentage that can give the optimum overall performance for all three queues. In the worst case scenario, drawn in Fig. 3 for the hybrid_15% curve, CoS0 delay can increase only up to about 7ms in contrast to that of WDSA resulting in an absolute value of 25ms. On the other hand, due to the same weight applied for all priority queues, an increase in delay up to 65ms

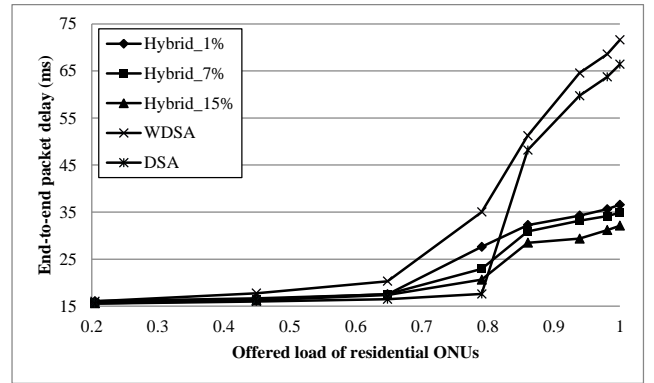


Fig. 4. End-to-end packet delay for CoS2 traffic.

is observed at the highest traffic load for CoS0 with DSA, as shown in Fig. 3. Similar performance was also obtained for CoS1 that is not presented in the paper. It is important to mention that these delays are still significantly below the potential limit of packet delay for mobile backhauling.

Finally, as shown in Fig. 4, the time insensitive class, CoS2, exhibits the lowest priority in accessing the network and, as a result, is expected to present the worst performance in packet delay. Different from before the hybrid algorithm over performs for the first time the competition as was initially observed in Fig. 3 and is confirmed here. The justification of this trend was also given as part of the analysis of Fig. 3 and results from the adaptive weights allowing more bandwidth to be allocated to CoS2 queues in the lower offered load range. In particular, at the offer load more than 0.78 the end-to-end packet delay of hybrid algorithm is 30ms compared to 74ms for WDSA. Similar performance to CoS0 is observed for DSA as expected following the same analysis presented for Fig. 3.

VI. CONCLUSION

The design, implementation and evaluation of an adaptive protocol and its associated algorithms that allow efficient control over the QoS experienced by LTE-A UEs, backhauled via an OFDMA-PON network have been presented. The first contribution of the paper is that original wireless models were developed in OPNET to demonstrate a practical LTE-A network and perform the mapping of wireless QCIs to OFDMA-PON CoSs. This converged network exhibits 20km reach, 32-split, 1024 subcarriers and 40Gbps aggregate rates with 16, 1Gbps eNB/ONUs, 16 residential ONUs and 10 UEs per eNB/ONU with 50km/h mobility.

Secondly with respect to mapping, a new mapping control element (MCE) was introduced in the developed eNB/ONUs to map QCI 5 to CoS0 (high priority), QCI 1, 2 to CoS1 (middle priority) and QCI 6, 7 to CoS2 (low priority). Thirdly, in relation to bandwidth allocation, intelligent traffic queuing, for intra-ONU allocation, and traffic-specific inter-ONU subcarrier allocation were implemented to demonstrate a fair distribution between the three priority queues as well as to guarantee the QoS of high-priority bearers. Adaptive algorithms were therefore evaluated, backed-up with analytical results that depending on the changing traffic conditions can optimize the subcarrier grouping ratio and assigned weights of each priority

queue, between a weighted and a non-weighted scheduler, to display an increased degree of fairness and therefore the accurate distribution of bandwidth among priority queues. To be able to implement this in practice, the hybrid protocol ensures that during the subcarrier assignment in the OLT, ONUs send an upstream REPORT message with the number of bytes in each of their OFDMA-PON CoS queues rather than the overall ONU request.

The hybrid algorithm was further compared to an algorithm with a fixed, 10:5:2 weight distribution, confirming that the fairness index of the adaptive algorithm is in all cases above 0.9. It has also been shown that the hybrid algorithm operating at an increased rate by the non-weighted scheduler, benefits the lower priority queues. This is an important result considering the performance of low priority packets, could increase above 100ms, imposing a potential limitation for mobile backhauling.

Concentration on, however, However for an ever increasing traffic, above 80%, adaptive weights start imposing higher delays for the high and middle priority queues. This occurs because in the hybrid algorithm any adaptation step on the subcarrier grouping ratio and weight parameters performs in favor of the non-weighted scheduler and as a whole in comparison to DSA, CoS0 might not have access to the amount of bandwidth provided before. This characteristic is not expected to impose a limitation in the converged network performance. The first reason is that it occurs while in parallel there is an improvement, of the low priority packets. Also, significantly, in the presence of the hybrid protocol the network can be automatically optimized to the adaptation step percentage that can give the optimum overall performance for all three queues.

REFERENCES

- [1] 3GPP, [Online]. Available at: www.3gpp.org/LTE
- [2] D. Astély, E. Dahlman, A. Furuskär, Y. Jading, M. Lindström, and S. Parkvall, "LTE: The Evolution of Mobile Broadband," *IEEE Commun. Mag.*, vol. 47, no. 4, pp. 44-51, April 2009.
- [3] A. Ghosh, R. Ratasuk, B. Mondal, N. Mangalvedhe, and T. Thomas, "LTE-advanced: next-generation wireless broadband technology [Invited Paper]," *IEEE Wireless Commun.*, vol. 17, no. 3, pp. 10-22, June 2010.
- [4] P. Bhat, S. Nagata, L. Campoy, I. Berberana, T. Derham, G. Liu, X. Shen, P. Zong and Jin Yang, "LTE-advanced: an operator perspective," *IEEE Commun. Mag.*, vol 50, no. 2, pp. 104-114, Feb. 2012
- [5] L.-C. Wang, S. Rangapillai, "A Survey on Green 5G Cellular Networks," *In Proc. Signal Processing and Communications (SPCOM) 2012*, July 2012.
- [6] A. Damjanovic, J. Montojo, C. Joonyoung, J. Hyounghu, Y. Jin, and Z. Pingping, "UE's role in LTE advanced heterogeneous networks," *IEEE Commun. Mag.*, vol. 50, pp. 164-176, Feb. 2012.
- [7] "Cisco Visual Networking Index (VNI) Global Mobile Data Traffic Forecast Update 2013," [Online] www.cisco.com
- [8] W. Lim, P. Kourtessis, M. Milosavljevic, and J. M. Senior, "QoS Mapping for LTE Backhauling over OFDMA-PONs," in *ProcICTON 2012*, June 2012, paper Tu.C3.2.
- [9] W. Lim, P. Kourtessis, M. Milosavljevic and J. M. Senior, "Optical and wireless convergence," in *Proc. OSA ANIC 2012*, June 2012, paper AW2A.5.
- [10] W. Lim, K. Kanonakis, P. Kourtessis, M. Milosavljevic, I. Tomkos, and J. M. Senior, "Flexible QoS Differentiation in Converged OFDMA-PON and LTE Networks," in *Proc. OFC/NFOEC 2013*, Mar. 2013 (In press)
- [11] W. Lim, K. Kanonakis, P. Kourtessis, M. Milosavljevic, I. Tomkos, and J. M. Senior, "Modeling of LTE back-hauling through OFDMA-PONs," in *Proc. ONDM 2013*, Apr. 2013.
- [12] EU FP7 COMBO project [Online], Available at: <http://www.ict-combo.eu/>
- [13] N. Cvijetic, "OFDM for Next-Generation Optical Access Networks," *Journal of Lightwave Technol.*, vol.30, no.4, pp.384-398, 2012.
- [14] K. Kanonakis, I. Tomkos, H. G. Krimmel, F. Schaich, C. Lange, E. Weis, J. Leuthold, M. Winter, S. Romero, P. Kourtessis, M. Milosavljevic, I. Cano, and J. Prat, "An OFDMA-Based Optical Access Network Architecture Exhibiting Ultra-High Capacity and Wireline-Wireless Convergence," *IEEE Commun. Mag.*, vol. 50, no. 8, pp. 71-78, Aug. 2012.
- [15] K. Kanonakis, E. Giacomidis, and I. Tomkos, "Physical Layer Aware MAC Schemes for Dynamic Subcarrier Assignment in OFDMA-PON Networks," *J. Lightwave Technol.*, vol. 30, no. 12, pp. 1915-1923, June 2012.
- [16] W. Lim, P. Kourtessis, M. Milosavljevic and J. M. Senior, "Dynamic Subcarrier Allocation for 100 Gbps, 40 km OFDMA-PONs with SLA and CoS," *J. Lightwave Technol.*, vol. 31, no. 7, pp. 1055-1062, Apr. 2013.
- [17] M.A. Ali et al., "On the Vision of Complete Fixed-Mobile Convergence," *J. Lightwave Technol.*, vol.28, no.16, pp.2343-2357, 2010.
- [18] G. Shen, R. S. Tucker and C.-J. Chae., "Fixed Mobile Convergence Architectures for Broadband Access: Integration of EPON and WiMAX," *IEEE Commun. Mag.*, vol.45, pp. 44-50, Aug. 2007.
- [19] K. Yang, S. Ou, K. Guild and H.-H. Chen, "Convergence of Ethernet PON and IEEE 802.16 Broadband Access Networks and its QoS-Aware Dynamic Bandwidth Allocation Scheme," *IEEE J. Sel. Areas Commun.*, vol. 27, pp. 101-116, Feb. 2009.
- [20] B. Jung, J. Choi, Y.-T. Han, M.-G. Kim and M. Kang, "Centralized Scheduling Mechanism for Enhanced End-to-End Delay and QoS Support in Integrated Architecture of EPON and WiMAX," *J. Lightwave Technol.*, vol. 28, pp. 2277-2288, Aug. 2010.
- [21] N. Madamopoulos, S. Peiris, N. Antoniadis, D. Richards, B. Pathak, G. Ellinas, R. Dorsinville, and M. A. Ali, "A Fully Distributed 10G-EPON-based Converged Fixed-Mobile Networking Transport Infrastructure for Next Generation Broadband Access," *J. Opt. Commun. Netw.*, vol. 4, no. 5, pp. 366-377, May 2012.
- [22] C. Ranaweera, E. Wong, C. Lim, and A. Nirmalathas, "Next Generation Optical-Wireless Converged Network Architectures," *IEEE Netw.*, vol. 26, no. 2, pp. 22-27, Mar./Apr. 2012.
- [23] 3GPP TS 36.321, "Evolved Universal Terrestrial Radio Access (E-UTRA) Medium Access Control (MAC) Protocol Specification".
- [24] 3GPP TS 23.203, "Policy and charging control architecture".
- [25] H. Ekstrom, "QoS control in the 3GPP evolved packet system," *IEEE Commun. Mag.*, vol. 47, pp. 76-83, Feb. 2009.
- [26] K. Kanonakis and I. Tomkos, "An Overview of MAC Issues in OFDMA-PON Networks [Invited]," in *Proc. ICTON'11*, 26-30 June 2011.
- [27] I.-S. Hwang and A. T. Liem, "Centralized Scheduling Mechanism for Enhanced End-to-End Delay and QoS Support in Integrated Architecture of EPON and WiMAX," *J. Lightwave Technol.*, vol. 31, no. 2, pp. 213-222, Jan. 2013.
- [28] M. C. Yuang, P.-L. Tien, D.-Z. Hsu, S.-Y. Chen, C.-C. Wei, J.-L. Shih, and J. Chen, "A High-Performance OFDMA PON System Architecture and Medium Access Control," *J. Lightwave Technol.*, vol. 30, no. 11, pp. 1685-1693, June 2012.